ARTICLE OPEN

Check for updates

Modulatory effects of ketamine on EEG source-based resting state connectivity in treatment resistant depression

Ty Lees[1,2], Jason N. Scott Jr[1], Brian W. Boyle[2,3], Shiba M. Esfand[1], Samantha R. Linton[1,2], Courtney Miller[3], Mohan Li[1], Sarah E. Woronko[1], Rebecca Dunayev[1], Mario Bogdanov[1,2], Paula Bolton[3], Shuang Li[2,3], Robert C. Meisner[3,4] and Diego A. Pizzagalli[1,2,5]✉

Treatment-resistant depression (TRD) accounts for approximately 30% of major depressive disorder cases and has been characterized by altered functional connectivity within and between the Default Mode (DMN) and Frontoparietal networks (FPN). Ketamine can be an effective treatment for TRD, and its antidepressant response has been associated with alterations in resting state functional connectivity (rsFC). Here, we evaluated the effect of a single subanesthetic dose of racemic ketamine (0.5 mg/kg) on electroencephalogram (EEG) derived source-based measures of rsFC from 24 participants with TRD (16 women; aged 44.35 ± 15.86 years). Ninety-six channel resting state EEG data were collected 24 h before and after ketamine infusion. Exact low-resolution electromagnetic tomography (eLORETA) was used to estimate theta and beta-band rsFC within and between the DMN and FPN. Ruminative symptoms were assessed using the Ruminative Response Scale. Analogous data were collected from 34 healthy control participants (25 women, aged 32.49 ± 14.07 years) who did not receive any intervention. Twenty-four hours post-infusion, depressive, anhedonic, and ruminative symptoms for the TRD sample were significantly reduced. Interestingly, symptom reduction was not correlated with any changes in rsFC but was associated with initial pre-ketamine rsFC. Moreover, individuals with TRD displayed broad increases in rsFC within the DMN and FPN as well as between these two networks. Based on preclinical findings, we posit that ketamine's synaptogenic effects may be driving this general increase in connectivity. However, these synaptogenic effects can be short lived, and future work probing the full time-course of rsFC via EEG pre- and post-ketamine administration is warranted.

Translational Psychiatry (2026)16:134; https://doi.org/10.1038/s41398-026-03928-4

INTRODUCTION

Major depressive disorder (MDD) is characterized by cognitive, emotional, and physical symptoms [1, 2]. Substantial clinical heterogeneity renders treating MDD challenging, evidenced by the fact that up to 50% of individuals with MDD do not benefit from first-line and subsequent antidepressant therapies [3]. Indeed, those not improving across at least two antidepressant trials (appropriate in dose, duration, and adherence) in their current episode are typically considered to suffer from treatment resistant depression (TRD), also known as difficult to treat depression [4]; these individuals account for approximately 30% of MDD cases [5]. Relative to individuals who benefit from antidepressant treatment, individuals with TRD experience negative outcomes including high relapse and hospitalization rates [6–8], highlighting urgent needs for different treatments.

Ketamine, a N-methyl-D-aspartate (NMDA) receptor antagonist, has emerged as an effective treatment for TRD [9, 10]. Two overlapping models posit ketamine's mechanism of action, the disinhibition and direct inhibition hypotheses [11–14]. The former suggests that ketamine preferentially blocks NMDA receptors on gamma amino butyric acid inhibitory (GABA) interneurons. These interneurons disinhibit the prefrontal cortex (PFC), increasing glutamate, leading to a sustained activation of α-amino-3-hydroxy-5-methyl-4-isoxazolepropionic acid (AMPA) receptors that triggers synaptic release of brain-derived neurotrophic factor (BDNF). BDNF binding then results in mammalian target of rapamycin (mTOR) mediated synaptogenesis [11, 15, 16]. The direct inhibition hypothesis, by contrast, suggests that ketamine directly antagonizes PFC NMDA receptors which directly cascade into similar synaptogenic pathways [11, 13, 17]. Notably, both hypotheses describe synaptogenesis as the final common pathway of ketamine's mechanism of action, and these alterations in connectivity might underlie its antidepressant effect [18].

MDD has been increasingly characterized as involving disrupted large-scale brain network connectivity, and research has generally centered on Menon's tripartite model of the Default Mode (DMN), Central Executive (i.e., Frontoparietal Network; FPN), and Salience Networks (SN) as a key pathophysiological framework [19–22]. TRD is no different, and recent reviews have suggested that altered connectivity within the DMN, and between the DMN and the FPN, as well as subcortical structures, may characterize TRD [23, 24]. More specifically, individuals with TRD exhibit within-DMN hyperconnectivity relative to those with MDD who benefit from antidepressant treatment and non-depressed controls [25, 26].

[1]Center for Depression, Anxiety, and Stress Research, McLean Hospital, Belmont, MA 02478, USA. [2]Department of Psychiatry, Harvard Medical School, Boston, MA 02215, USA. [3]Psychiatric Neurotherapeutics Program, McLean Hospital, Belmont, MA 02478, USA. [4]Acute Psychiatric Service, Massachusetts General Hospital, Boston, MA 02114, USA. [5]Noel Drury, M.D. Institute for Translational Depression Discoveries, University of California Irvine, Irvine, CA 92617, USA. ✉email: dpizzaga@hs.uci.edu

Received: 8 August 2025 Revised: 17 February 2026 Accepted: 20 February 2026
Published online: 06 March 2026

Several subcortical structures including the amygdala, hippocampus, and habenula and their connectivity with cortical DMN loci have also been implicated in TRD [27–29]. Importantly, Ma et al. [30] noted that patterns of connectivity differentiate individuals with TRD from treatment-responsive individuals and posited that node-specific approaches may be important for understanding treatment resistance.

Recent research has probed these assumptions by using measures of neural connectivity to understand ketamine's antidepressant effects (see [31–33] for recent reviews), and treatment-related changes in rsFC have emerged [34]. Indeed, several studies have found that ketamine alters global brain connectivity of the PFC (which includes key DMN, FPN, and SN structures) [35, 36], with node-based analyses suggesting that ketamine reduces within-PFC connectivity and enhances PFC connectivity to other brain regions [35, 37]. Notably, one study demonstrated increased global brain connectivity in the DMN and FPN [38], echoing other fMRI-based connectivity studies that implicate similar regions and networks [25, 39, 40]. That said, it is worth noting that some global connectivity work has failed to find any relationship between PFC connectivity and antidepressant response in MDD participants, despite observing reduced baseline connectivity in these participants [41]. The authors postulate that study- (e.g., scan interval) or subject-related variables (e.g., sex distribution) may account for these results, however, it is also possible that changes in PFC connectivity may not index ketamine's antidepressant response.

Complementing hemodynamic neuroimaging, electrophysiological metrics can also be used to index functional connectivity [42, 43]; however, only a limited number of studies have used such approaches to probe the effects of ketamine. Studies using magnetoencephalography (MEG) to estimate source connectivity have found that ketamine exposure is associated with significant reductions in connectivity between specific nodes (e.g., the insulo-temporal nodes and the amygdala, and a precentral cortical network and the subgenual anterior cingulate cortex; [44]), and more widely across the brain [45]. Notably, these more widespread reductions in connectivity did not correlate with antidepressant response, even though other connectivity parameters did distinguish between those who were and were not responsive to ketamine [45]. Indeed, several studies using electroencephalography (EEG) provided similar results and have shown reduced connectivity in frontal structures for those benefitting from ketamine [46], as well as increased connectivity in visual cortices [47] and AMPA-related frontoparietal signaling [48].

Notably, while EEG-based measures of connectivity have been used to examine depression-related treatment outcomes (e.g., [49–51]), to the best of our knowledge, these examinations have not included ketamine. McMillan and colleagues' [52] analysis of simultaneously captured EEG and fMRI data provides a possible starting point, whereby widespread changes in source-based spectral power estimates during ketamine infusion were identified, though these changes did not predict antidepressant response. These changes reflect alterations to the underlying neural oscillations but notably, do not index functional connectivity between neural networks. Thus, the primary goal of the present study was to evaluate the effect/s of a single subanesthetic dose of racemic ketamine (0.5 mg/kg) on EEG-derived source-based measures of rsFC. Based on previous literature, we hypothesized that, 24 h post-infusion, ketamine would: 1) reduce depressive, anhedonic, and ruminative symptoms; 2) decrease within-DMN connectivity; 3) increase within-FPN connectivity; and 4) decrease connectivity between the DMN and FPN.

MATERIALS AND METHODS

The broader study of which the present data were part was registered on ClinicalTrials.gov, NCT04239963, and was carried out at McLean Hospital, Belmont, Massachusetts.

Participants

Prior to the start of the study, we estimated the necessary sample size based on the results of relevant neuroimaging literature. An integrative analysis of 9 ketamine trials found that ketamine elicits medium-to-large reductions in depressive symptoms when compared to midazolam (Cohen's $d = 0.70$) and saline ($d = 1.60$), and that the pooled 24-hour response rate (i.e., percentage of individuals with a more than 50% reduction in symptoms) was 46% [53]. Using this information, we found that at a two-tailed α of 0.05 and a mean effect size of 1.15, $n = 30$ TRD participants will be associated with a power > 0.85 to detect changes after ketamine injection, differences between responders and non-responders, and identify baseline EEG and/or behavioral markers predicting treatment response.

Thirty-six people with TRD scheduled for ketamine therapy were recruited from McLean Hospital's Ketamine Service. Prior to enrolment, participants completed a screening session where their diagnosis was confirmed using the Mini International Neuropsychiatric Interview (MINI; [54]) and symptoms assessed using several questionnaires (see Supplement) including the Hamilton Depression Rating Scale (HAMD; [55]), the Quick Inventory of Depression Scale (QIDS; [56]), the Mood and Anxiety Symptom Questionnaire (MASQ; [57]), and the Snaith-Hamilton Pleasure Scale (SHAPS; [58]). Forty-three additional participants were screened via the MINI to be psychologically healthy and serve as a control group (HC), which led to 2 HC participants being excluded (see Supplement for Inclusion/Exclusion criteria). Furthermore, 11 participants (2 HC and 9 TRD) withdrew prior to EEG data collection, 6 participants (3 HC and 3 TRD) were lost to follow up, and data from 2 HC participants were excluded due to excessive EEG artifacts.

Thus, the final EEG sample consisted of 24 participants with TRD (16 women, aged 44.35 ± 15.86 years) and 34 HC participants (25 women, aged 32.49 ± 14.07 years). The two groups were similar in their education and sex distribution (p's ≥ 0.704). However, TRD participants were, on average, older than HC participants ($t(1,45.79) = -2.94$, $p = 0.005$), and more likely to self-identify as white ($\chi^2 = 12.17$, $p = 0.002$). A detailed demographic description of both groups is presented in Supplementary Table 1; notably, all TRD subjects were medicated (see Supplementary Table 2) and did not change medications across the study sessions.

Study procedure

Study procedures were approved by the Mass General Brigham Institutional Review Board, and participants provided written informed consent. All study procedures were performed in accordance with the relevant guidelines and regulations. Participants were compensated for their time, and those in the TRD group had their first ketamine dose paid for by the study.

Eligible participants completed two study sessions separated by 48 h; individuals with TRD were tested 24-hours before and after their first ketamine infusion, and healthy participants waited the 48-hour period without any intervention. At both sessions, participants completed the HAMD, QIDS, SHAPS, and the Ruminative Response Scale (RRS; [59]), as well as an EEG protocol described below.

EEG protocol and recording

Continuous EEG data were recorded using a 96-channel equidistant spherical actiCAP and actiChamp amplifier (Brain Products GmbH, Gilching, Germany) digitized at 500 Hz using BrainVision Recorder Software (v1.25.0201; Brain Products GmbH). Data were referenced online to the vertex channel with a ground electrode located approximately at AFz, and impedances were maintained below 25 KΩ.

Both sessions began with recording 8-min of resting EEG data in 1-min segments. Four minutes were recorded with eyes open and four minutes with eyes closed; the order of which was randomized and counterbalanced across participants. This resting baseline was followed by two tasks (not reported here). Consistent with our previous studies investigating EEG-based functional connectivity [50, 60, 61], only eyes-closed resting EEG data were analyzed.

EEG preprocessing

EEG data were processed using BrainVision Analyzer (v2.2; Brain Products GmbH). Raw data were first visually inspected to remove gross muscle artifacts and identify artifactual channels. Data were then filtered between 1–100 Hz using a second-order Butterworth zero-phase IIR filter. Next, independent component analysis was used to remove components

Table 1. Clinical symptoms for healthy controls and TRD participants at both testing sessions.

Scale	Group	T1 Mean (SD)	T2 Mean (SD)	*t*	*df*	*p*
Depression						
HAMD	HC	0.34 (0.79)	0.15 (0.57)	1.44	30	0.161
	TRD	15.58 (4.96)	11.41 (5.7)	2.75	21	0.012[a]
QIDS	HC	0.16 (0.45)	0.18 (0.58)	−1.00	30	0.325
	TRD	13.86 (4.29)	9.68 (4.76)	2.80	19	0.011[a]
Anhedonia						
SHAPS	HC	18.26 (4.99)	19.06 (5.65)	−1.56	33	0.129
	TRD	37.46 (5.79)	35.29 (5.88)	2.13	23	0.044[a]
Rumination						
RRS – Total	HC	28.83 (5.02)	27.68 (4.71)	2.33	29	0.027[a]
	TRD	64.78 (9.09)	60.42 (9.84)	3.16	22	0.005[a]
RRS – Brooding	HC	6.58 (1.54)	6.38 (1.44)	1.76	30	0.088
	TRD	14.43 (2.86)	13.33 (2.70)	2.21	22	0.038[a]
RRS – Depression	HC	15.19 (2.55)	14.29 (2.37)	2.49	31	0.018[a]
	TRD	38.67 (5.02)	35.42 (5.59)	2.95	23	0.007[a]
RRS – Reflection	HC	7.36 (2.64)	7.00 (1.91)	1.36	32	0.184
	TRD	12.12 (3.66)	11.67 (3.69)	1.80	23	0.086

HAMD Hamilton Depression Rating Scale, *HC* Healthy Control, *QIDS* Quick-Inventory of Depression, *RRS* Ruminative Response Scale, *SHAPS* Snaith-Hamilton Pleasure Scale, T1 Testing Session 1, *T2* Testing Session 2, *TRD* Person with Treatment Resistant Depression.
[a] = Statistical Significance.

containing artifact sources (e.g., eyeblinks and movements, cardiac and muscle signals). Artifactual channels were interpolated using spherical splines [62], and data were re-referenced to the common average. Non-overlapping 2048 ms segments were then extracted for functional connectivity analyses. The lowest number of segments exported was 105 corresponding to at least 215 sec of data, a value beyond the recommended minimum 40 sec [63]. Moreover, the average number of segments did not differ between HCs and TRDs at session 1 (116.38 ± 1.56 vs. 118.04 ± 7.29; $t = -1.098$, $p = 0.283$) or session 2 (117.06 ± 3.13 vs. 118.25 ± 5.14; $t = -1.010$, $p = 0.319$). Finally, the number of segments did not differ between sessions for both groups (p's ≥ 0.27).

eLORETA measures and quantification

Functional connectivity estimates were computed using eLORETA implemented via the LORETA software (v20221219; [63]). eLORETA is a linear inverse problem solution capable of correctly reconstructing localized cortical activity from scalp-recorded data. It uses a solution space of 6239 cortical gray matter voxels embedded in the realistic head model [64] from the Montreal Neurological Institute 152 template [65]. Several studies validated the original LORETA algorithm [66–68], and the eLORETA algorithm has been validated using MEG [69, 70] and EEG combined with MRI [71].

Functional connectivity was estimated using lagged phase synchronization (LPS; see Supplement). LPS quantifies the nonlinear relationship between two regions of interest (ROI) after removing instantaneous EEG connectivity, which likely reflects volume conduction effects [63]. Based on prior hypotheses and findings in independent MDD samples [50, 60], LPS was estimated across several ROIs within the DMN and FPN. We elected to focus on these two networks due to their inclusion in Menon's tripartite model of psychopathology [21], and their possible roles in the pathophysiology of depression generally [20, 22] and treatment-resistant depression [23, 24]. ROIs were defined using seed points from our previous MDD studies [50, 60] and included all gray matter voxels within a 10 mm radius; details for all ROI seeds are listed in Supplementary Table 3.

Normalized Fourier transforms applied to all artifact-free segments of data were used to calculate the LPS between ROIs in the following frequency bands: theta (4.5–7 Hz), beta1 (12.5–18 Hz), beta2 (18.5–21 Hz), and beta3 (21.5–30 Hz). Analyses were confined to these frequency bands as: 1) recent reviews of relevant oscillatory and connectivity EEG analyses highlight the theta, beta, and gamma frequency bands as relevant to depression and ketamine treatment of depression [33, 72, 73] and; 2) previous EEG-based rsFC studies from our laboratory have implicated theta and beta band connectivity in depression and its treatment [50, 60, 61]. Finally, at the suggestion of an anonymous reviewer, we also examined global lagged connectivity to further contextualise our ROI specific approach; these results are presented in the Supplement.

Data analysis

Analytically, we evaluated *Group*, *Session*, and *Group* × *Session* differences in within- and between-network connectivity by simultaneously comparing LPS between all pairs of ROIs at each frequency. Within-group between-*Session* change was evaluated using dependent sample t-tests, while the between-*Group* within-session and the *Group* × *Session* differences were evaluated using independent sample t-tests assuming unequal variances. All tests were submitted to non-parametric permutations based on the maximal statistic [74, 75] with 5000 randomizations to correct for multiple comparisons. Additionally, to further probe group-level differences in LPS, we also evaluated these tests using a t-value threshold that corresponded to an uncorrected $p < 0.005$; The respective t-values that corresponded to an uncorrected $p < 0.005$ were 3.009 and 3.105 for the HC and TRD within-group comparisons, and 2.923 for the between-group comparison.

Moreover, as age significantly differed between the two groups, we used ordinary least squares regression models to evaluate any identified significant *Group* or *Group* × *Session* differences when also controlling for age. These models estimated the main effect of age at session 1 (mean centered to the full population mean), and either the *Group* or *Group* × *Session* effect. To account for possible extreme values, LPS parameters were winsorized at the 5th and 95th percentile prior to analyses.

Lastly, we conducted a bivariate correlation analysis to examine the associations between change in LPS and change in rumination scores in TRD participants, as well as between initial LPS and change in rumination.

RESULTS

First, we evaluated if depressive symptoms changed between sessions (Table 1). As hypothesized, depressive symptoms of individuals with TRD significantly decreased between sessions when assessed by the HAMD (15.58 ± 4.96 vs. 11.48 ± 5.70; $t = -2.754$, $p = 0.012$) and the QIDS (13.86 ± 4.29 vs. 9.68 ± 4.76; $t = -2.799$, $p = 0.011$). The HAMD and QIDS scores of HC participants did not differ between testing sessions (p's ≥ 0.161) Similar results were observed when examining anhedonic

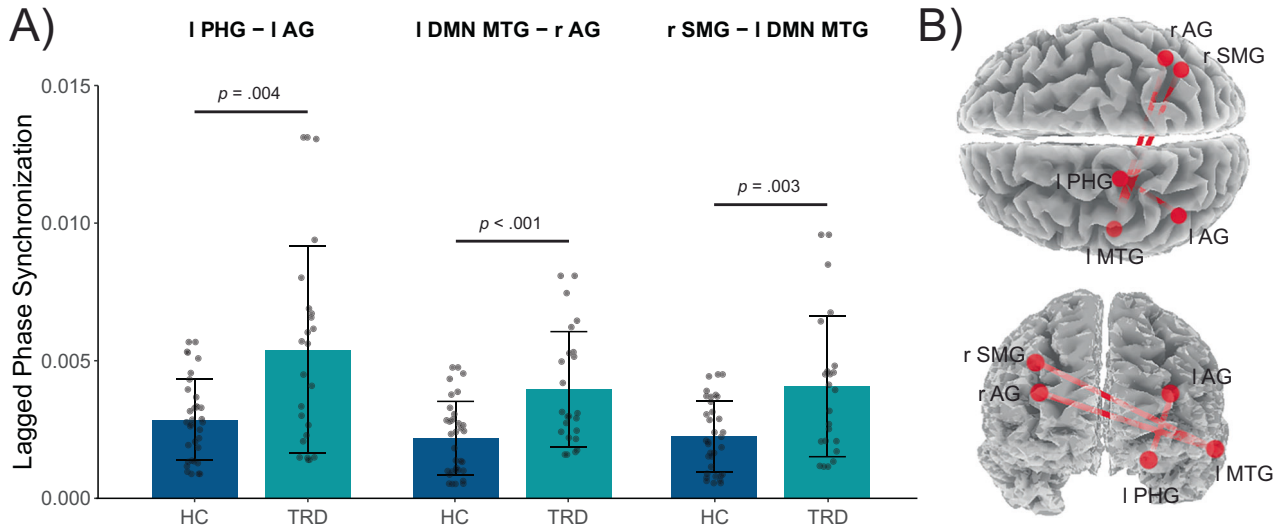

Fig. 1 Beta3 lagged phase synchronization for healthy controls and TRD participants at testing session 1. Note: Plot A presents the beta 3 LPS values for the ROI pairs/connections that significantly differed between groups (i.e., healthy controls and TRD participants) at session 1. LPS values were winsorized before plotting and are plotted as the Mean ± SD (error bars); all other connections did not significantly differ between the two groups and have not been plotted for clarity. Plot B localizes these connections within the Colin-27 MNI brain volume. AG Angular Gyrus, DMN Default Mode Network, HC Healthy Control, l Left, LPS Lagged Phase Synchronization, MTG Mid-temporal Gyrus, PHG Parahippocampal Gyrus, r Right, SMG Supramarginal Gyrus, TRD Treatment Resistant Depression, * Statistical significance.

symptoms (SHAPS scores) where TRD participants reported a small but significant reduction (37.46 ± 5.79 vs 35.29 ± 5.88; $t = -2.126$, $p = 0.044$), while HC participants reported no change ($p = 0.129$). Moreover, we observed that the total rumination scores of TRD participants significantly decreased between the two sessions (64.78 ± 9.09 vs. 60.42 ± 9.84, $t = -3.161$, $p = 0.005$), as did their scores on the brooding ($t = -2.206$, $p = 0.038$) and depression-related rumination ($t = -2.953$, $p = 0.007$) subscales. Interestingly, the HC group also showed a significant reduction in their total ($t = -2.332$, $p = 0.027$) and depression-related rumination ($t = -2.487$, $p = 0.018$); however, these decreases were notably smaller than for the TRD participants (3.98% vs. 6.73% and 5.93% vs. 8.40%). Finally, neither group significantly changed in their reflective thinking (p's ≥ 0.086).

Group differences in functional connectivity

Next, we compared LPS between the two groups at session 1 (Fig. 1), i.e., prior to TRD participants receiving treatment. Significant group differences emerged in beta3 within-DMN connectivity. Specifically, relative to HC, participants with TRD had significantly higher LPS between the left parahippocampal gyrus and left angular gyrus ($t = 3.009$) and left mid-temporal gyrus and right angular gyrus ($t = 3.313$); both effects were retained after controlling for age ($t = 3.167$, $p = 0.003$; and $t = 2.771$, $p = 0.008$).

In addition, we also observed a difference in beta3 DMN-FPN connectivity, where people with TRD exhibited greater right supramarginal gyrus and left mid-temporal gyrus LPS when compared to HC ($t = 3.239$; Fig. 1). This effect, again, survived when controlling for age ($t = 2.577$, $p = 0.013$).

Change in functional connectivity between groups

The next step was to probe the *Group* × *Session* interaction term, i.e., group differences in the change in LPS (ΔLPS) between sessions.

Within-Network. Within the FPN, participants with TRD showed significantly greater ΔLPS relative to HCs. More specifically, TRD participants were characterized by greater change in theta precuneus to left supramarginal gyrus connectivity ($t = 2.974$; Fig. 2A/B), and beta2 right to left supramarginal gyri connectivity ($t = 3.181$; Fig. 2C/D). Both effects remained when controlling for age ($t = 3.691$, $p < 0.001$; and $t = 3.032$, $p = 0.004$).

Turning to the DMN, participants with TRD showed a significantly larger change in beta2 connectivity between the right parahippocampal gyrus and left superior frontal gyrus ($t = 3.109$), and the right and left angular gyri ($t = 2.991$; Fig. 2E/F). These group differences were confirmed after controlling for age ($t = 2.870$, $p = 0.006$; and $t = 2.841$, $p = 0.006$).

Between-Network. With respect to DMN-FPN connectivity, we observed several significant group differences in the degree of theta, beta1, and beta2 ΔLPS, such that TRD participants showed significantly greater changes relative to HCs. More specifically, TRD participants had greater change in: theta band precuneus and left angular gyrus connectivity ($t = 3.483$; Fig. 3A/B); beta1 band paracingulate gyrus and right superior frontal gyrus connectivity ($t = 3.017$; Fig. 3C/D); and beta2 band connectivity between the right supramarginal gyrus and left angular gyrus ($t = 3.595$; Fig. 3E/F), and the right mid-temporal gyrus and left parahippcampal gyrus ($t = 3.036$). Each of these effects remained after controlling for age (t's = ≥ 2.846, p's ≤ 0.006).

Session-related differences in functional connectivity

After examining the *Group* × *Session* effect, we then evaluated the between-session differences in rsFC of the TRD group. We observed that DMN-FPN beta2 connectivity between the right supramarginal gyrus and the left angular gyrus ($t = 3.215$) and between the left frontoparietal mid-temporal gyrus and the right angular gyrus ($t = 3.148$) significantly increased (Fig. 4A/B). Probing the connections implicated in the *Group* × *Session* analysis provided further evidence for increases in DMN-FPN connectivity, identifying a significant rise in precuneus and left angular gyrus theta band connectivity ($t = 2.591$, $p = 0.016$), and in right frontoparietal mid-temporal gyrus and right angular gyrus beta2 band connectivity ($t = 2.831$, $p = 0.009$).

The *Group* × *Session* follow-up analysis also revealed between-session increases in within-network connectivity. Within the DMN, beta2 connectivity increased between the right parahippocampal gyrus and left superior frontal gyrus ($t = 2.506$, $p = 0.020$), and between the left and right angular gyri ($t = 2.499$, $p = 0.020$).

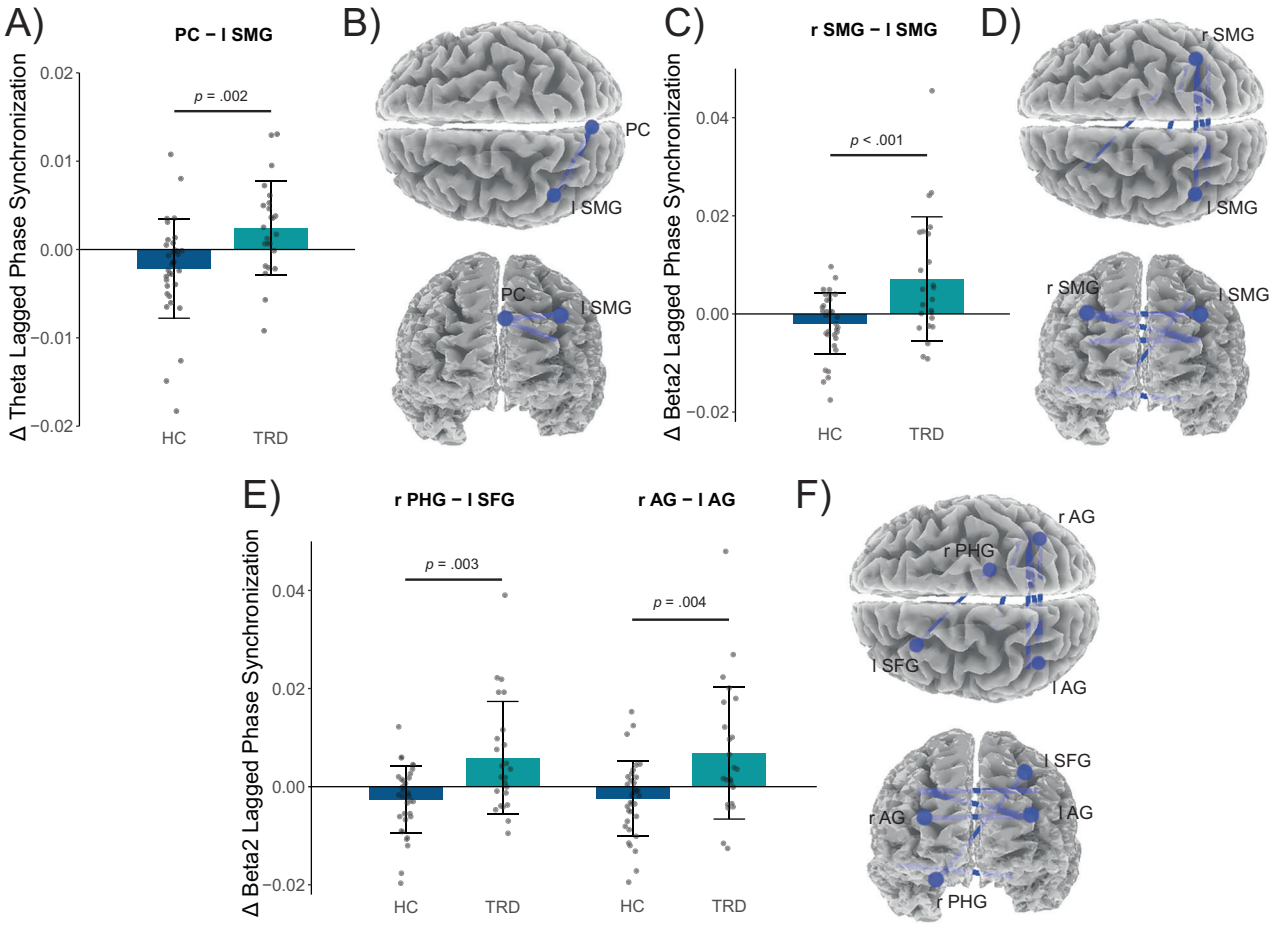

Fig. 2 Differences in the between-session change in within-network connectivity between the healthy control and TRD groups. Note: Plot A presents the change in theta LPS values (computed as the session 1 LPS value subtracted from the session 2 LPS value) for the within-FPN connection that significantly differed in the degree of between session change between the HC and TRD groups. Plots C and E present analogous change in beta2 LPS data for connections within the FPN and DMN, respectively. LPS values were winsorized before plotting and are plotted as the Mean ± SD (error bars); all other connections did not significantly differ and are not plotted for clarity. Plots B, D, and F localizes these connections within the Colin-27 MNI brain volume. AG Angular Gyrus, DMN Default-Mode Network, FPN Frontoparietal Network, HC Healthy Controls, l Left, LPS Lagged Phase Synchronization, PC Precuneus, PHG Parahippocampal Gyrus, r Right, SFG Superior Frontal Gyrus, SMG Supramarginal Gyrus, TRD Treatment Resistant Depression, * Statistical significance.

Within the FPN, precuneus and left supramarginal gyrus theta connectivity increased ($t = 2.257$, $p = 0.034$) as did beta2 connectivity between the right and left supramarginal ($t = 2.752$, $p = 0.011$).

Associations between changes in LPS and ruminative thinking

Finally, we examined if any implicated ΔLPS parameter was significantly associated with changes in HAMD and RRS scores among TRD participants. The correlation analysis revealed no significant association between ΔLPS of any implicated connections and change in HAMD score (r's ≤ |0.16|, p's ≥ 0.48), total rumination score (r's ≤ |0.27|, p's ≥ 0.24), brooding score (r's ≤ |0.32|; p's ≥ 0.13), and depression-related rumination score (r's ≤ |0.24|, p's ≥ 0.28). Interestingly, change in right parahippocampal gyrus and the left superior frontal gyrus beta2 connectivity (i.e., within-DMN connectivity) was positively associated with change in reflective thinking ($r = 0.41$, $p = 0.04$), such that a greater increase in connectivity predicted a greater increase in reflective thinking; all other associations were not significant (r's ≤ |0.39|, p's ≥ 0.06).

In addition, we also conducted an exploratory correlation analysis that used session 1 LPS values rather than ΔLPS; these results are presented in Table 2. In contrast to the ΔLPS correlations, we observed significant positive associations between changes in total ruminative thinking and connectivity within the DMN ($r = 0.520$, $p = 0.016$) and within the FPN ($r = 0.478$, $p = 0.029$), such that greater reductions in rumination were associated with reduced rsFC at session 1. Notably, these associations appear to be largely driven by depression-related ruminative thinking which showed a similar pattern of significance (right column of Table 2; r's ≥ 0.434, p's ≤ 0.044), rather than brooding and reflecting thinking where no significant associations with any LPS value were observed (p's ≥ 0.06).

DISCUSSION

The present study evaluated rsFC changes associated with the first dose of ketamine among individuals with TRD. In line with our hypothesis and existing literature, within 24-hours, ketamine significantly reduced depressive, anhedonic, and ruminative symptoms. Interestingly, while demonstrating the expected pre-treatment elevation in DMN connectivity relative to their HC counterparts, we observed that the rsFC of patients with TRD demonstrated a broad increase following ketamine infusion. More specifically, in contrast to our hypotheses, we observed an increase in within-DMN beta2 connectivity, as well as increased theta and beta DMN-FPN connectivity. We did, however, observe the expected increase in within-FPN connectivity. Notably, these

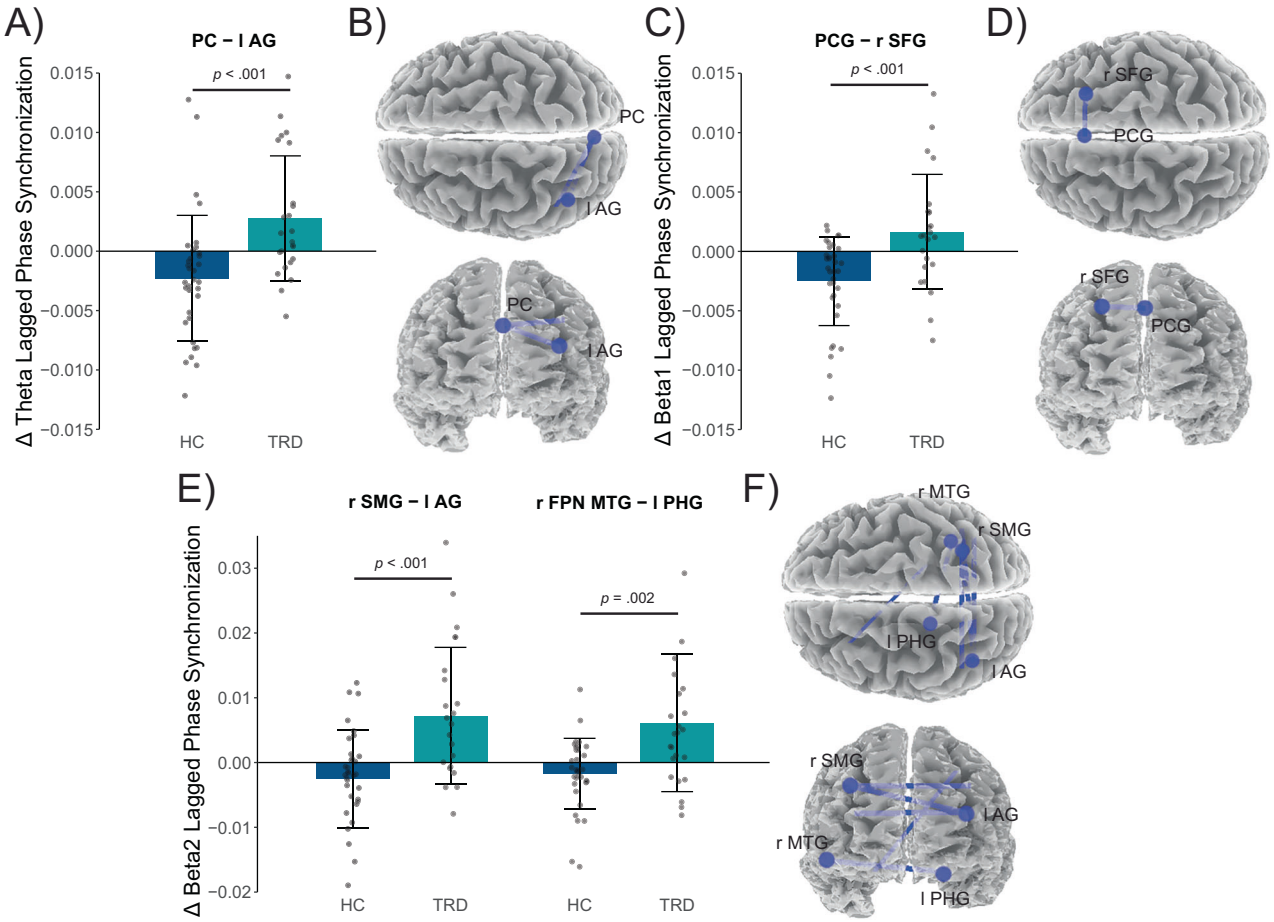

Fig. 3 Differences in the between-session change in between-network connectivity between the healthy control and TRD groups. Note: Plot A presents the change in theta LPS values (computed as the session 1 LPS value subtracted from the session 2 LPS value) for the FPN-DMN connection that significantly differed in the degree of between session change between the HC and TRD groups. Plots C and E present analogous change in LPS data for beta1 and beta2 frequency bands, respectively. LPS values were winsorized before plotting and are plotted as the Mean ± SD (error bars); all other connections did not significantly differ and are not plotted for clarity. Plots B, D, and F localize these connections within the Colin-27 MNI brain volume. AG Angular Gyrus, DMN Default Mode Network, FPN Frontoparietal Network, HC Healthy Control, l Left, LPS Lagged Phase Synchronization, MTG Mid-temporal gyrus, PC Precuneus, PCG Paracingulate Gyrus, PHG Parahippocampal Gyrus, SMG Supramarginal Gyrus, TRD Treatment Resistant Depression, * Statistical significance.

ROI-specific effects contrasted with the observed reduction in theta, beta2, and beta3 global lagged connectivity (see Supplementary Results). Together, these results suggest that ketamine acutely and broadly modifies neural connectivity but may have unique effects within depression-relevant brain regions, aligning with existing imaging and preclinical literature.

Pre-treatment hyperconnectivity within the DMN and between the DMN and FPN in individuals with TRD, relative to their HC counterparts, is consistent with meta-analytic evidence from fMRI studies [20, 23, 24]. Interestingly, the implicated within-DMN ROI pairs involve, among other nodes, the angular gyri. The cortical regions of these gyri are thought to be involved in integrating multimodal information for subsequent processing [78] and have key roles in self-referential cognition and autobiographical memory [79, 80]. These functions might that explain why initial rsFC (i.e., LPS at session 1) in several ROI pairs that included the angular gyri were significantly associated with change in depression-related rumination. The nature of these correlations suggests that those with the greatest ketamine-related antidepressant response were characterized by reduced connectivity within the DMN and FPN, as well as between the two networks. It is possible that such changes could guide future research that proactively uses EEG-based measures of rsFC in guiding antidepressant therapy. However, capturing 96-channel EEG data and subsequent eLORETA analysis requires more technical expertise, and thus refinements to the data collection procedure are warranted.

Beyond these initial differences in connectivity, given ketamine's antidepressant effects, it might be surmised that ketamine would also reduce the within-DMN and DMN-FPN hyperconnectivity and increase the within-FPN hypoconnectivity often observed in MDD and TRD [20, 23, 24]; accordingly, the observed broad rsFC increase among individuals with TRD following their first ketamine infusion is also largely unexpected. That said, prior EEG studies have reported increased connectivity in and between frontoparietal and visual cortices following ketamine [47, 48], suggesting that the specific neural nodes implicated may define the direction of change. Nonetheless, following the mechanisms of action described by the disinhibition and direct inhibition hypotheses, we speculate that the observed increases in connectivity represent an initial spike in synaptogenesis [11]. Preclinical work using a mouse model of depression supports this notion and has shown that ketamine restores functional connectivity in the cortex and does so by both recovering lost dendritic spines and triggering de novo spineogenesis (i.e., the formation of spines in new dendritic locations) that initializes somewhere between 6–12 h post-exposure and peaks around 24-hours post-exposure [81].

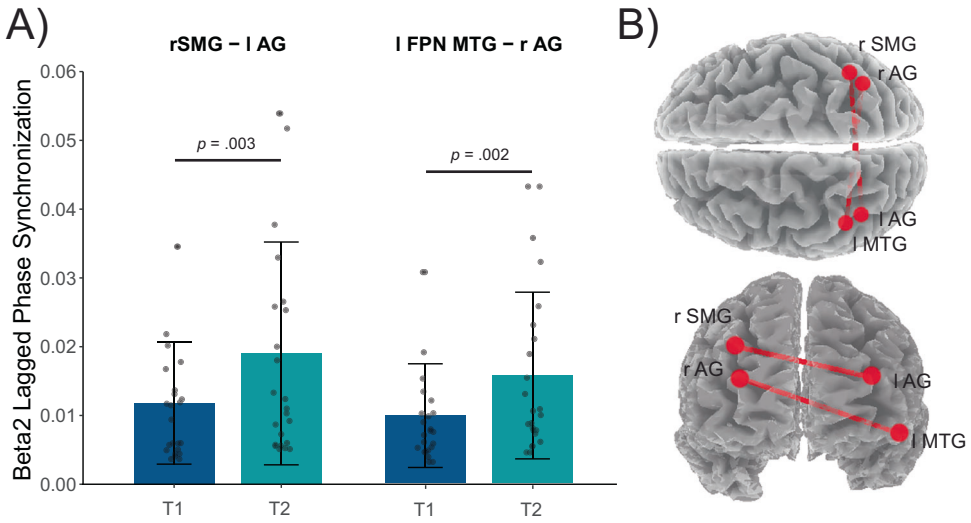

Fig. 4 Between testing session change in lagged phase synchronization of the TRD participants. Note: Plots A presents the beta2 LPS values for connections that differed for the TRD group. LPS values were winsorized before plotting and are plotted as the Mean ± SD (error bars); all other connections did not significantly differ and are not plotted for clarity. Plot B localizes these connections within the Colin-27 MNI brain volume. AG Angular gyrus, FPN Frontoparietal Network, l Left LPS Lagged Phase Synchronization, MTG Midtemporal Gyrus, r Right, SMG Supramarginal Gyrus, T1 Testing Session 1, T2 Testing Session 2, * Statistical significance.

Table 2. Zero-order associations between change in ruminative thinking scores and initial within- and between-network lagged phase synchronization of TRD participants.

	Δ Total Rumination Score		Δ Depression-Related Rumination	
	r	p	r	p
θ PC – l AG	0.080	0.731	−0.198	0.378
θ PC – l SMG	0.140	0.544	−0.124	0.583
β_2 l FPN MTG – r AG	0.469	0.032	0.479	0.024[a]
β_2 r SMG – l AG	0.427	0.053	0.434	0.044[a]
β_2 r PHG – l SFG	0.148	0.521	0.225	0.315
β_2 r AG – l AG	0.520	0.016[a]	0.587	0.004[a]
β_2 r SMG – l SMG	0.478	0.029[a]	0.468	0.028[a]
β_2 r FPN MTG – l PHG	0.335	0.137	0.586	0.004[a]

Change in Hamilton Depression Rating Scale Score as well as Ruminative Brooding and Reflective thinking were not significantly associated with any LPS value and are not presented for clarity.
AG Angular Gyrus, *FPN* Frontoparietal Network, *l* Left, *LPS* Lagged Phase Synchronization, *MTG* Mid-temporal gyrus, *PC* Precuneus, *PHG* Parahippocampal Gyrus, *r* Right, *SFG* Superior Frontal Gyrus, SMG Supramarginal Gyrus, TRD Treatment Resistant Depression, *θ* theta band, *β2* beta2 band.
[a] = Statistical significance.

Additionally, Moda-Sava et al. [81] note that a majority (~55%) of newly formed dendritic spines are lost within four days of ketamine exposure which suggests some form of pruning process. It may be that following this pruning we would observe the expected patterns of change in functional connectivity, i.e., reduced DMN and DMN-FPN connectivity accompanied by increased FPN connectivity. With this in mind, we would encourage any future research to record EEG at multiple timepoints following ketamine administration to evaluate this hypothesis. Of note, for many, without additional doses, depressive symptoms often re-emerge within approximately one week of ketamine treatment [82, 83], and maintenance of antidepressant effects typically requires repeated, sometimes long-term, dosing. Indeed, most existing studies of the brain-based correlates of ketamine's antidepressant response have only examined the effect of a single infusion [33]. Thus, conducting a study that evaluates changes in rsFC across the full time-course of ketamine treatment (e.g., pre-infusion, during infusion, 4–24 h post infusion, and 2–7 days post-infusion for all infusions in a treatment program), may identify alterations in connectivity across different timescales (i.e., immediate vs. long-term) and of different types (i.e., transient vs. stable) and provide greater ability to understand ketamine-related treatment outcomes and responsivity. Similarly, while our specific goal was to evaluate putative changes in rsFC 24-hours post-infusion, ketamine's antidepressant effects emerge rapidly within a few hours post-infusion [84] and significant synaptic changes occur within the first 24 h [81]. Moreover, EEG informed fMRI analysis has demonstrated the existence of different time-courses of ketamine-induced neural changes [52], and so, it is possible that a denser sampling around/during ketamine infusions would provide more insight into the dynamics of ketamine's effects on rsFC.

Finally, we examined if any of the implicated changes in rsFC were correlated with change in depressive symptoms. In contrast to our hypothesis, there were no significant associations between these parameters, although this is perhaps not too unexpected when considered from the synaptogenic framework discussed above. Moda-Sava et al., [81] observed a timing disconnect between ketamine's behavioral and synaptogenic effects (i.e., 3-hours vs. 12–24 h post exposure), as well as no association between spine formation and immobility behavior (i.e., a depressive symptom homologue for rodents). These results align with some prior human research that also observed no such associations (e.g., [45, 52]) and suggest that synaptogenesis may only be important for sustaining ketamine's antidepressant effect not initiating it. Perhaps then the present lack of correlations is more the result of where in time rsFC parameters were assessed rather than the true absence of said association suggesting the need for future verification studies. Related to depressive symptoms, beyond the expected changes in TRD participants, the ruminative scores of HC participants also significantly decreased between session. This effect could be related to measurement variability, however, given that the RRS was a self-report scale, we would suggest that it is more likely a result of the confined variance in rumination scores for HCs, i.e., minimized variance renders differences of smaller magnitudes (e.g., the

observed mean change in depressive rumination for HCs was less than 1 point) more likely to be statistically significant. Nonetheless, this is something for future research to consider when evaluating change in depressive symptoms.

Looking ahead, while the present study focused on intravenous racemic ketamine, future EEG studies might consider similar assessment before and after intranasal delivery of esketamine which has similar antidepressant effects [85]. This could also be combined with adding a placebo-controlled group of participants with TRD and a sham treatment group for HC as well as adjusting to a cross-over design, all of which would better enable causal analyses regarding ketamine's effects on neural connectivity and overcome an important limitation of the present study. Furthermore, the availability of FDA-approved esketamine for psychiatric indications may also allow recruitment of larger samples, increasing statistical power, and thus navigating a challenge faced by ROI-based connectivity studies (i.e., the number of statistical tests conducted). That said, while modest, our sample size of $n = 24$ TRD participants is well aligned with existing literature, whereby across 34 relevant electrophysiological studies of functional connectivity in depression and its treatment included in recent reviews the average number of participants with depression included in the analysis was approximately 22 people [33, 72].

When speaking to our sample, it is worth considering other possible sources of group differences. As previously noted, TRD subjects were, on average, older than their HC counterparts and all self-identified as White. While our analysis controlled for effects of age, it did not factor in racial identity. This was, in part, because it would lead to subgroups too small for meaningful analyses, and because we had no a priori hypothesis of how LPS and change in LPS would be affected by race. Nonetheless, we know that race-related socioenvironmental factors can have neurobiological effects [86] and larger follow-up studies should factor the racial identity of their subjects into their analytical approach. Additionally, TRD participants were all medicated (Supplementary Table 2) and it is possible that this may also affect neural connectivity. As such, the inclusion of a group of unmedicated TRD participants, while challenging for several reasons (e.g., washout procedures, ethical requirements of care) would help future research to further specify ketamine's effects.

Finally, to focus specifically on future directions for EEG-based functional connectivity, while we constrained our analysis to the theta and beta frequencies based on a synthesis of several reviews and empirical studies, Miljevic et al., [72] note several studies have observed alpha-band connectivity effects relevant to depression. Alpha-based EEG parameters, most often alpha asymmetry, have been regularly used in depression-research [87] and so, future studies should consider evaluating if connectivity at the alpha frequencies are meaningful targets. Moreover, such studies may also consider adding task-based measures of functional connectivity to supplement any resting-state findings. The design structure and standardized nature of typical EEG tasks could potentially be used to constrain the neural processes and associated systems activated and subsequently directly target networks of interest, i.e., the DMN, FPN, and/or SN.

In sum, we evaluated the effect of ketamine on EEG-derived source-based measures of DMN and FPN rsFC in individuals with TRD. Within 24-hours of their first infusion, individuals with TRD showed significant reductions in depressive, anhedonic, and ruminative symptoms. Moreover, they were characterized by broad increases in functional connectivity within the DMN and FPN as well as between the two networks. Based on preclinical evidence, we speculate such general connectivity increases might be driven by ketamine's synaptogenic effects. Because preclinical models suggest that these synaptogenic effects can decline rapidly, an important next step will be to use EEG to track the full time-course of ketamine therapy, starting prior to the first infusion and following through all subsequent doses.

DATA AVAILABILITY

The data used in the present work are available upon reasonable request to the corresponding author.

CODE AVAILABILITY

We used the following software in preprocessing the raw EEG data and the subsequent analysis: BrainVision Analyzer (v2.2), LORETA (v20221219) via its graphical interface; *R* (v4.3.0) [76] using R-Studio (v2023.06.0.421) [77], and the *stats* (v4.3.0) [76] R package. The R code and EEG preprocessing templates are available from the corresponding author on reasonable request.

REFERENCES

1. Herrman H, Patel V, Kieling C, Berk M, Buchweitz C, Cuijpers P, et al. Time for united action on depression: A Lancet–World Psychiatric Association Commission. The Lancet. 2022;399:957–1022.
2. American Psychiatric Association Diagnostic and Statistical Manual of Mental Disorders. 5th ed.. American Psychiatric Association; 2013.
3. Taylor RW, Marwood L, Greer B, Strawbridge R, Cleare AJ. Predictors of response to augmentation treatment in patients with treatment-resistant depression: A systematic review. J Psychopharmacol. 2019;33:1323–39.
4. Gaynes BN, Lux L, Gartlehner G, Asher G, Forman-Hoffman V, Green J, et al. Defining treatment-resistant depression. Depress Anxiety. 2020;37:134–45.
5. McIntyre RS, Alsuwaidan M, Baune BT, Berk M, Demyttenaere K, Goldberg JF, et al. Treatment-resistant depression: definition, prevalence, detection, management, and investigational interventions. World Psychiatry. 2023;22:394–412.
6. Johnston KM, Powell LC, Anderson IM, Szabo S, Cline S. The burden of treatment-resistant depression: A systematic review of the economic and quality of life literature. J Affect Disord. 2019;242:195–210.
7. Zhdanava M, Pilon D, Ghelerter I, Chow W, Joshi K, Lefebvre P, et al. The prevalence and national burden of treatment-resistant depression and major depressive disorder in the United States. J Clin Psychiatry. 2021;82:20m13699.
8. Ivanova JI, Birnbaum HG, Kidolezi Y, Subramanian G, Khan SA, Stensland MD. Direct and indirect costs of employees with treatment-resistant and non-treatment-resistant major depressive disorder. Curr Med Res Opin. 2010;26:2475–84.
9. Smith-Apeldoorn SY, Veraart JK, Spijker J, Kamphuis J, Schoevers RA. Maintenance ketamine treatment for depression: a systematic review of efficacy, safety, and tolerability. Lancet Psychiatry. 2022;9:907–21.
10. McIntyre RS, Rosenblat JD, Nemeroff CB, Sanacora G, Murrough JW, Berk M, et al. Synthesizing the evidence for ketamine and esketamine in treatment-resistant depression: An international expert opinion on the available evidence and implementation. Am J Psychiatry. 2021;178:383–99.
11. Aleksandrova LR, Wang YT, Phillips AG. Hydroxynorketamine: Implications for the NMDA receptor hypothesis of ketamine's antidepressant action. Chronic Stress. 2017;1:2470547017743511.
12. Aleksandrova LR, Phillips AG. Neuroplasticity as a convergent mechanism of ketamine and classical psychedelics. Trends Pharmacol Sci. 2021;42:929–42.
13. Miller OH, Moran JT, Hall BJ. Two cellular hypotheses explaining the initiation of ketamine's antidepressant actions: Direct inhibition and disinhibition. Neuropharmacology. 2016;100:17–26.
14. Abdallah CG, Sanacora G, Duman RS, Krystal JH. Ketamine and rapid-acting antidepressants: A window into a new neurobiology for mood disorder therapeutics. Annu Rev Med. 2015;66:509–23.
15. Maeng S, Zarate CA, Du J, Schloesser RJ, McCammon J, Chen G, et al. Cellular mechanisms underlying the antidepressant effects of ketamine: role of α-Amino-3-Hydroxy-5-Methylisoxazole-4-Propionic acid receptors. Biol Psychiatry. 2008;63:349–52.
16. Gerhard DM, Pothula S, Liu R-J, Wu M, Li X-Y, Girgenti MJ, et al. GABA interneurons are the cellular trigger for ketamine's rapid antidepressant actions. J Clin Invest. 2020;130:1336–49.
17. Kavalali ET, Monteggia LM. Synaptic mechanisms underlying rapid antidepressant action of ketamine. Am J Psychiatry. 2012;169:1150–6.
18. Duman RS, Aghajanian GK, Sanacora G, Krystal JH. Synaptic plasticity and depression: new insights from stress and rapid-acting antidepressants. Nat Med. 2016;22:238–49.
19. Northoff G. How do resting state changes in depression translate into psychopathological symptoms? From 'Spatiotemporal correspondence' to 'Spatiotemporal Psychopathology'. Curr Opin Psychiatry. 2016;29:18–24.
20. Kaiser RH, Andrews-Hanna JR, Wager TD, Pizzagalli DA. Large-Scale network dysfunction in major depressive disorder. JAMA Psychiatry. 2015;72:603.
21. Menon V. Large-scale brain networks and psychopathology: a unifying triple network model. Trends Cogn Sci. 2011;15:483–506.

22. Northoff G. Spatiotemporal psychopathology I: No rest for the brain's resting state activity in depression? Spatiotemporal psychopathology of depressive symptoms. J Affect Disord. 2016;190:854–66.
23. Runia, Yücel DE N, Lok A, de Jong K, Denys DAJP, van Wingen GA, et al. The neurobiology of treatment-resistant depression: A systematic review of neuroimaging studies. Neurosci Biobehav Rev. 2022;132:433–48.
24. Grehl MM, Hameed S, Murrough JW. Brain features of treatment-resistant depression. Psychiatric Clinics of North America. 2023;46:391–401.
25. Siegel JS, Palanca BJA, Ances BM, Kharasch ED, Schweiger JA, Yingling MD, et al. Prolonged ketamine infusion modulates limbic connectivity and induces sustained remission of treatment-resistant depression. Psychopharmacology (Berl). 2021. 22 January 2021. https://doi.org/10.1007/s00213-021-05762-6.
26. Sun J, Ma Y, Guo C, Du Z, Chen L, Wang Z, et al. Distinct patterns of functional brain network integration between treatment-resistant depression and non treatment-resistant depression: A resting-state functional magnetic resonance imaging study. Prog Neuropsychopharmacol Biol Psychiatry. 2023;120:110621.
27. Lui S, Wu Q, Qiu L, Yang X, Kuang W, Chan RCK, et al. Resting-State functional connectivity in treatment-resistant depression. Am J Psychiatry. 2011;168:642–8.
28. Barreiros AR, Breukelaar I, Mayur P, Andepalli J, Tomimatsu Y, Funayama K, et al. Abnormal habenula functional connectivity characterizes treatment-resistant depression. Neuroimage Clin. 2022;34:102990.
29. Amiri S, Arbabi M, Kazemi K, Parvaresh-Rizi M, Mirbagheri MM. Characterization of brain functional connectivity in treatment-resistant depression. Prog Neuropsychopharmacol Biol Psychiatry. 2021;111:110346.
30. Ma C, Ding J, Li J, Guo W, Long Z, Liu F, et al. Resting-State functional connectivity bias of middle temporal gyrus and caudate with altered gray matter volume in major depression. PLoS ONE. 2012;7:e45263.
31. Zavaliangos-Petropulu A, Al-Sharif NB, Taraku B, Leaver AM, Sahib AK, Espinoza RT, et al. Neuroimaging-Derived biomarkers of the antidepressant effects of ketamine. Biol Psychiatry Cogn Neurosci Neuroimaging. 2023;8:361–86.
32. Yun J-Y, Kim Y-K. Neural correlates of treatment response to ketamine for treatment-resistant depression: A systematic review of MRI-based studies. Psychiatry Res. 2024;340:116092.
33. Medeiros GC, Matheson M, Demo I, Reid MJ, Matheson S, Twose C, et al. Brain-based correlates of antidepressant response to ketamine: a comprehensive systematic review of neuroimaging studies. Lancet Psychiatry. 2023;10:790–800.
34. Medeiros GC, Demo I, Goes FS, Zarate CA, Gould TD. Personalized use of ketamine and esketamine for treatment-resistant depression. Transl Psychiatry. 2024;14:481.
35. Abdallah CG, Averill LA, Collins KA, Geha P, Schwartz J, Averill C, et al. Ketamine treatment and global brain connectivity in major depression. Neuropsychopharmacology. 2017;42:1210–9.
36. Abdallah CG, Dutta A, Averill CL, McKie S, Akiki TJ, Averill LA, et al. Ketamine, but not the NMDAR antagonist lanicemine, increases prefrontal global connectivity in depressed patients. Chronic Stress. 2018;2:2470547018796102.
37. Abdallah CG, Ahn K-H, Averill LA, Nemati S, Averill CL, Fouda S, et al. A robust and reproducible connectome fingerprint of ketamine is highly associated with the connectomic signature of antidepressants. Neuropsychopharmacology. 2021;46:478–85.
38. Moujaes F, Ji JL, Rahmati M, Burt JB, Schleifer C, Adkinson BD, et al. Ketamine induces multiple individually distinct whole-brain functional connectivity signatures. eLife. 2024;13:e84173.
39. Mkrtchian A, Evans JW, Kraus C, Yuan P, Kadriu B, Nugent AC, et al. Ketamine modulates fronto-striatal circuitry in depressed and healthy individuals. Mol Psychiatry. 2021;26:3292–301.
40. Evans JW, Szczepanik J, Brutsché N, Park LT, Nugent AC, Zarate CA. Default mode connectivity in major depressive disorder measured up to 10 days after ketamine administration. Biol Psychiatry. 2018;84:582–90.
41. Kraus C, Mkrtchian A, Kadriu B, Nugent AC, Zarate CA, Evans JW. Evaluating global brain connectivity as an imaging marker for depression: influence of preprocessing strategies and placebo-controlled ketamine treatment. Neuropsychopharmacology. 2020;45:982–9.
42. Mantini D, Perrucci MG, Del Gratta C, Romani GL, Corbetta M. Electrophysiological signatures of resting state networks in the human brain. Proc Natl Acad Sci. 2007;104:13170–5.
43. Chang C, Liu Z, Chen MC, Liu X, Duyn JH. EEG correlates of time-varying BOLD functional connectivity. Neuroimage. 2013;72:227–36.
44. Nugent AC, Robinson SE, Coppola R, Zarate CA. Preliminary differences in resting state MEG functional connectivity pre- and post-ketamine in major depressive disorder. Psychiatry Res Neuroimaging. 2016;254:56–66.
45. Nugent AC, Ballard ED, Gilbert JR, Tewarie PK, Brookes MJ, Zarate CA. The effect of ketamine on electrophysiological connectivity in major depressive disorder. Front Psychiatry. 2020;11:519.
46. Minami S, Kato M, Ikeda S, Yoshimura M, Ueda S, Koshikawa Y, et al. Association between the rostral anterior cingulate cortex and anterior insula in the salience network on response to antidepressants in major depressive disorder as revealed by isolated effective coherence. Neuropsychobiology. 2022;81:475–83.
47. Sumner RL, McMillan R, Spriggs MJ, Campbell D, Malpas G, Maxwell E, et al. Ketamine enhances visual sensory evoked potential long-term potentiation in patients with major depressive disorder. Biol Psychiatry Cogn Neurosci Neuroimaging. 2020;5:45–55.
48. Sumner RL, McMillan RL, Forsyth A, Muthukumaraswamy SD, Shaw AD. Neurophysiological evidence that frontoparietal connectivity and GABA-A receptor changes underpin the antidepressant response to ketamine. Transl Psychiatry. 2024;14:116.
49. Rolle CE, Fonzo GA, Wu W, Toll R, Jha MK, Cooper C, et al. Cortical connectivity moderators of antidepressant vs placebo treatment response in major depressive disorder. JAMA Psychiatry. 2020;77:397.
50. Whitton AE, Webb CA, Dillon DG, Kayser J, Rutherford A, Goer F, et al. Pretreatment rostral anterior cingulate cortex connectivity with salience network predicts depression recovery: Findings from the EMBARC randomized clinical trial. Biol Psychiatry. 2019;85:872–80.
51. Choi K-M, Lee T, Im C-H, Lee S-H. Prediction of pharmacological treatment efficacy using electroencephalography-based salience network in patients with major depressive disorder. Front Psychiatry. 2024;15:1469645.
52. McMillan R, Sumner R, Forsyth A, Campbell D, Malpas G, Maxwell E, et al. Simultaneous EEG/fMRI recorded during ketamine infusion in patients with major depressive disorder. Prog Neuropsychopharmacol Biol Psychiatry. 2020;99:109838.
53. Wilkinson ST, Farmer C, Ballard ED, Mathew SJ, Grunebaum MF, Murrough JW, et al. Impact of midazolam vs. saline on effect size estimates in controlled trials of ketamine as a rapid-acting antidepressant. Neuropsychopharmacology. 2019;44:1233–8.
54. Sheehan DV, Lecrubier Y, Sheehan KH, Amorim P, Janavs J, Weiller E, et al. The Mini-International Neuropsychiatric Interview (M.I.N.I.): The development and validation of a structured diagnostic psychiatric interview for DSM-IV and ICD-10. J Clin Psychiatry. 1998;59:22–33.
55. Hamilton M. A rating scale for Depression. J Neurol Neurosurg Psychiatry. 1960;23:56–62.
56. Rush AJ, Trivedi MH, Ibrahim HM, Carmody TJ, Arnow B, Klein DN, et al. The 16-Item quick inventory of depressive symptomatology (QIDS), clinician rating (QIDS-C), and self-report (QIDS-SR): a psychometric evaluation in patients with chronic major depression. Biol Psychiatry. 2003;54:573–83.
57. Clark LA, Watson D. Tripartite model of anxiety and depression: Psychometric evidence and taxonomic implications. J Abnorm Psychol. 1991;100:316–36.
58. Snaith RP, Hamilton M, Morley S, Humayan A, Hargreaves D, Trigwell P. A scale for the assessment of hedonic tone the Snaith–Hamilton pleasure scale. Br J Psychiatry. 1995;167:99–103.
59. Nolen-Hoeksema S, Morrow J. A prospective study of depression and posttraumatic stress symptoms after a natural disaster: The 1989 Loma Prieta earthquake. J Pers Soc Psychol. 1991;61:115–21.
60. Whitton AE, Deccy S, Ironside ML, Kumar P, Beltzer M, Pizzagalli DA. Electroencephalography source functional connectivity reveals abnormal high-frequency communication among large-scale functional networks in depression. Biol Psychiatry Cogn Neurosci Neuroimaging. 2018;3:50–8.
61. Lees T, Woronko SE, Li M, Scott JN, Kuhn M, Esfand SM, et al. Differences in high-frequency connectivity among large-scale functional networks linked to major depressive disorder and treatment-resistant depression. Biol Psychiatry Global Open Sci. 2025;5:100602.
62. Perrin F, Pernier J, Bertrand O, Echallier JF. Spherical splines for scalp potential and current density mapping. Electroencephalogr Clin Neurophysiol. 1989;72:184–7.
63. Pascual-Marqui RD, Lehmann D, Koukkou M, Kochi K, Anderer P, Saletu B, et al. Assessing interactions in the brain with exact low-resolution electromagnetic tomography. Philos Trans Royal Soc A: Math Phys Eng Sci. 2011;369:3768–84.
64. Fuchs M, Kastner J, Wagner M, Hawes S, Ebersole JS. A standardized boundary element method volume conductor model. Clin Neurophysiol. 2002;113:702–12.
65. Mazziotta J, Toga A, Evans A, Fox P, Lancaster J, Zilles K, et al. A probabilistic atlas and reference system for the human brain: International Consortium for Brain Mapping (ICBM). Philos Trans R Soc Lond B Biol Sci. 2001;356:1293–322.
66. Mulert C, Jäger L, Schmitt R, Bussfeld P, Pogarell O, Möller H-J, et al. Integration of fMRI and simultaneous EEG: Towards a comprehensive understanding of localization and time-course of brain activity in target detection. Neuroimage. 2004;22:83–94.
67. Vitacco D, Brandeis D, Pascual-Marqui R, Martin E. Correspondence of event-related potential tomography and functional magnetic resonance imaging during language processing. Hum Brain Mapp. 2002;17:4–12.
68. Worrell GA, Lagerlund TD, Sharbrough FW, Brinkmann BH, Busacker NE, Cicora KM, et al. Localization of the epileptic focus by low-resolution electromagnetic tomography in patients with a lesion demonstrated by MRI. Brain Topogr. 2000;12:273–82.

69. Cao L, Thut G, Gross J. The role of brain oscillations in predicting self-generated sounds. Neuroimage. 2017;147:895–903.
70. Tan H-RM, Gross J, Uhlhaas PJ. MEG—measured auditory steady-state oscillations show high test–retest reliability: A sensor and source-space analysis. Neuroimage. 2015;122:417–26.
71. Liu Q, Farahibozorg S, Porcaro C, Wenderoth N, Mantini D. Detecting large-scale networks in the human brain using high-density electroencephalography. Hum Brain Mapp. 2017;38:4631–43.
72. Miljevic A, Bailey NW, Murphy OW, Perera MPN, Fitzgerald PB. Alterations in EEG functional connectivity in individuals with depression: A systematic review. J Affect Disord. 2023;328:287–302.
73. Newson JJ, Thiagarajan TC. EEG frequency bands in psychiatric disorders: A review of resting state studies. Front Hum Neurosci. 2019;12:521.
74. Nichols TE, Holmes AP. Nonparametric permutation tests for functional neuroimaging: A primer with examples. Hum Brain Mapp. 2002;15:1–25.
75. Holmes AP, Blair RC, Watson JDG, Ford I. Nonparametric analysis of statistic images from functional mapping experiments. J Cereb Blood Flow Metab. 1996;16:7–22.
76. R Core Team. R: A language and environment for statistical computing. R Foundation for Statistical Computing, Vienna, Austria. https://www.R-project.org/. 2025.
77. Posit team. RStudio: Integrated Development Environment for R. Posit Software PBC, Boston, USA. https://www.posit.co/ 2025.
78. Vatansever D, Manktelow AE, Sahakian BJ, Menon DK, Stamatakis EA. Angular default mode network connectivity across working memory load. Hum Brain Mapp. 2017;38:41–52.
79. Mizrahi T, Axelrod V. Similarity in activity and laterality patterns in the angular gyrus during autobiographical memory retrieval and self-referential processing. Brain Struct Funct. 2023;228:219–38.
80. Axelrod V, Rees G, Bar M. The default network and the combination of cognitive processes that mediate self-generated thought. Nat Hum Behav. 2017;1:896–910.
81. Moda-Sava RN, Murdock MH, Parekh PK, Fetcho RN, Huang BS, Huynh TN, et al. Sustained rescue of prefrontal circuit dysfunction by antidepressant-induced spine formation. Science (1979). 2019;364:eaat8078.
82. Zarate CA, Singh JB, Carlson PJ, Brutsche NE, Ameli R, Luckenbaugh DA, et al. A randomized trial of an N-methyl-D-aspartate Antagonist in treatment-resistant major depression. Arch Gen Psychiatry. 2006;63:856.
83. Ibrahim L, DiazGranados N, Franco-Chaves J, Brutsche N, Henter ID, Kronstein P, et al. Course of improvement in depressive symptoms to a single intravenous infusion of ketamine vs add-on riluzole: Results from a 4-Week, double-blind, placebo-controlled study. Neuropsychopharmacology. 2012;37:1526–33.
84. Serafini G, Howland R, Rovedi F, Girardi P, Amore M. The role of ketamine in treatment-resistant depression: A systematic review. Curr Neuropharmacol. 2014;12:444–61.
85. Papakostas GI, Salloum NC, Hock RS, Jha MK, Murrough JW, Mathew SJ, et al. Efficacy of esketamine augmentation in major depressive disorder. J Clin Psychiatry. 2020;81:19r12889.
86. Harnett NG, Merrill LC, Fani N. Racial and ethnic socioenvironmental inequity and neuroimaging in psychiatry: A brief review of the past and recommendations for the future. Neuropsychopharmacology. 2025;50:3–15.
87. Fitzgerald PJ. Frontal alpha asymmetry and its modulation by monoaminergic neurotransmitters in depression. Clin Psychopharmacol Neurosci. 2024;22:405–15.

ACKNOWLEDGEMENTS

Funding for this project was provided by an investigator-initiated contract from Millennium Pharmaceuticals (awarded to D.A.P).

AUTHOR CONTRIBUTIONS

Conceptualization: D.A.P., R.C.M. Methodology: D.A.P. Formal Analysis: T.L. Investigation: J.N.S. Jr., S.M.E., M.L., S.E.W. Resources: D.A.P. Data Curation: T.L., S.R.L., R.D. Writing – Original Draft: T.L. Writing – Review & Editing: T.L., J.N.S.Jr., S.M.E., M.L., S.E.W., S.R.L., R.D., M.B., B.W.B., C.M., P.B., S.L., R.C.M., D.A.P. Visualisation: T.L. Supervision: D.A.P. Project Administration: D.A.P. Funding Acquisition: D.A.P.

COMPETING INTERESTS

Over the past 3 years, Dr. Pizzagalli has received consulting fees from Abbvie, Arrowhead Pharmaceuticals, Boehringer Ingelheim, Circular Genomics, Compass Pathways, Engrail Therapeutics, N1 Biocorp Inc, Neumora Therapeutics, Neurocrine Biosciences, Neuroscience Software, Takeda, TP Sciences, and Xenon Pharmaceuticals; he has received honoraria from the American Psychological Association, Psychonomic Society and Springer (for editorial work) and Alkermes; he has received research funding from the Bird Foundation, Brain and Behavior Research Foundation, Circular Genomics, Dana Foundation, Millennium Pharmaceuticals, NIMH, and Wellcome Leap; he has received stock options from Ceretype Neuromedicine, Compass Pathways, Engrail Therapeutics, Neumora Therapeutics, and Neuroscience Software. All other authors have no conflicts of interest or relevant disclosures. All views expressed are solely those of the authors.

ADDITIONAL INFORMATION

Supplementary information The online version contains supplementary material available at https://doi.org/10.1038/s41398-026-03928-4.

Correspondence and requests for materials should be addressed to Diego A. Pizzagalli.

Supplementary Materials

Supplementary Methods

Inclusion and Exclusion Criteria

The inclusion criteria for the healthy control (HC) participants were as follows:

1. All genders, races, and ethnic origins.
2. Aged between 18 and 70 years.
3. Absence of medical, neurological, and psychiatric illness (including alcohol and substance abuse), as assessed by subject history and the Mini International Neuropsychiatric Inventory (MINI) interview.
4. A baseline Quick Inventory of Depression Scale (QIDS) score less than or equal to 5.
5. A baseline Hamilton Depression Rating Scale (HAMD) score less than or equal to 7.
6. Capable of providing written informed consent and fluent in English.
7. No first-degree relative with mood or psychotic disorder.

The inclusion criteria for the participants with treatment resistant depression (TRD) were as follows:

1. All genders, races, and ethnic origins.
2. Aged between 18 and 70 years.
3. Currently meet DSM-5 diagnostic criteria for Major Depressive Disorder (MDD) as assessed via the MINI.
4. A baseline HAMD (17-item version) score greater than 16, or a QIDS score greater than 12 and a Beck Depression Inventory - II score greater than 14.
5. Capable of providing written informed consent, and fluent in English.
6. Treatment Resistant as assessed via the Massachusetts General Hospital Antidepressant Response Questionnaire.
7. Have already decided to receive ketamine treatment as part of their standard clinical care.

Finally, the following exclusion criteria applied to all participants regardless of their group designation:

1. Any serious or unstable medical illness, including cardiovascular, hepatic, renal, respiratory, endocrine, neurologic or hematologic disease.
2. History of seizure disorder.

3. History or current diagnosis of any of the following DSM-5 psychiatric illnesses: schizophrenia, schizoaffective disorder, delusional disorder, psychotic disorders not otherwise specified.
4. Current diagnosis of substance use disorder.
5. Clinical or laboratory evidence of hypothyroidism, hyperthyroidism, or other thyroid disorder that is not controlled by medication.
6. Substance use assessed by physician as dangerous for ketamine treatment.
7. Untreated glaucoma.
8. Complex PTSD with dissociation.
9. Patients treated with electroconvulsive therapy (ECT) in the past 2 weeks.
10. Participants with a lifetime history of previous ketamine use.

Hamilton Depression Rating Scale (HAMD)

The HAMD [1] used here was the 17-item version assessing the severity of depressive symptoms over the past week. Most items are scored using values ranging from 0 to 4, while a few items use 3 scoring levels from 0 to 2. Overall scores range from 0 to 52 where higher scores indicate greater depression severity.

Mood and Anxiety Symptom Questionnaire (MASQ)

The MASQ is a self-report questionnaire designed to assess the tripartite model of anxiety and depression across the last week [2]. In this study the short-form (62-item) of the MASQ was used. Items are scored using a 1 (*not at all*) to 5 (*extremely*) rating scale to assess general distress depressive symptoms, general distress anxious symptoms, anxious arousal, and anhedonic depression. Scales are scored such that higher scores indicate greater symptom severity.

Quick Inventory of Depression Scale (QIDS)

The QIDS [3] is a 16-item measure derived from the Inventory of Depressive Symptomatology; the present study used the clinical administered measure. The QIDS evaluates of depressive symptom severity across the 9 DSM-IV symptom criterion domains of depression – including sad mood, concentration, self-criticism, suicidal ideation, interest, energy/fatigue, sleep disturbance, changes in appetite/weight, and psychomotor

agitation/retardation, where items are scored on a 4-point scale from 0 to 3 and total scores range from 0 to 27 with higher scores indicating greater symptom severity.

Snaith-Hamilton Pleasure Scale (SHAPS)

The SHAPS [4] is a 14-item self-report scale assesses loss of interest in or pleasure from completing everyday activities. Participants rate each item on a scale from 1 (*strongly agree*) to 4 (*strongly disagree*) as to how relevant the item was to themselves over the last few days. Overall scores range from 14 to 56 and are scored such that higher scores indicate higher levels of anhedonia.

Ruminative Response Scale (RRS)

The RRS [5] is a 22-item self-report scale that assesses a participant's overall ruminative thinking as well as subscales related to reflective thinking, brooding, and depression-related rumination. Participants rate each item on a 1 (*almost never*) to 4 (*almost always*) scale relevant to their thoughts when they feel down, sad, or depressed. Overall scores range from 22 to 88 and are scored such that higher scores indicate higher levels of rumination.

Lagged Phase Synchronization

Lagged phase synchronization (LPS) is a measure of non-linear intracortical functional connectivity calculated using normalized Fourier transforms [6]. In its derivation LPS minimizes the effects of volume conduction and associated artifacts by removing the instantaneous (i.e., zero-lag) component from the total phase synchronization parameter and leaving only the non-instantaneous (i.e., lagged) phase synchrony information. Total phase synchronization is computed using the following formula:

$$\varphi_{x,y}^2(\omega) = |f_{x,y}(\omega)|^2 = \left\{\mathrm{Re}\left[f_{x,y}(\omega)\right]\right\}^2 + \left\{\mathrm{Im}\left[f_{x,y}(\omega)\right]\right\}^2 \quad (1)$$

where:

$$f_{x,y}(\omega) = \frac{1}{N_R}\sum_{k=1}^{N_R}\left[\frac{x_k(\omega)}{|x_k(\omega)|}\right]\left[\frac{y_k^*(\omega)}{|y_k(\omega)|}\right] \quad (2)$$

In these equations, x and y represent the two regions of interest (ROIs) in the connectivity pair (i.e., the EEG sources) evaluated at a given discrete frequency, ω. In equation 1, *Re* and *Im* are the real and the imaginary parts of a complex element *C*, respectively; notably, zero-lag connectivity is closed related to *Re*. Equation 2 explains the cycle of *C*, where $x(\omega)$ and $y(\omega)$ denote the discrete Fourier transform of the two signals of interest, and * denotes a

complex conjugate (i.e., the inversion of the sign of only the imaginary part of a complex number).

From this description of total phase synchronization, LPS (i.e., non-instantaneous phase synchronization), is defined using the following formula:

$$\varphi_{x,y}^2(\omega) = \frac{\{\mathrm{Im}[f_{x,y}(\omega)]\}^2}{1 - \{\mathrm{Re}[f_{x,y}(\omega)]\}^2} \tag{3}$$

and measures the similarity of the phases of two time-series and is thought to contain only physiological connectivity information. Interpretatively, a value of 0 indicates no synchronization and a value of 1 indicates perfect synchronization.

Supplemental Table 1 – Demographic and clinical characteristics at initial study screening of both healthy controls and TRD participants.

	HC (n = 34)	TRD (n = 24)	t / χ^2	*df*	*p*
Demographics					
Female, n (%)	25 (73.53)	16 (66.67)	0.07	1	.785
Age, years, mean (SD)	32.49 (14.07)	44.35 (15.86)	-2.94	45.79	.005*
Education, years, mean (SD)	16.00 (3.98)	16.42 (4.15)	-0.38	48.41	.704
White, n (%)	22 (64.71)	24 (100)			
Black/African American, n (%)	1 (2.94)	0 (0)	12.17	2	.002*
Asian, n (%)	11 (32.35)	0 (0)			
Clinical Characteristics					
Number of MDEs, mean (SD)	–	5.00 (6.40)	–	–	–
Age at first MDE, mean (SD)	–	16.61 (4.69)	–	–	–
Episodes per year since first MDE, mean (SD)	–	0.25 (0.33)	–	–	–
Taking antidepressant (%)	0 (0)	24 (100)			
Depression and Ruminative Symptomatology					
HAMD	0.27 (0.57)	17.09 (5.71)	-14.07	22.31	< .001*
QIDS	0.18 (0.46)	15.22 (3.98)	-18.05	22.42	< .001*
SHAPS – Total	19.32 (5.90)	38.61 (5.52)	-12.58	49.41	< .001*
MASQ – AA	18.00 (1.83)	31.74 (9.42)	-6.90	23.20	< .001*
MASQ – GDA	12.61 (1.80)	29.96 (9.29)	-9.02	24.26	< .001*
MASQ – GDD	13.97 (3.30)	47.62 (6.21)	-24.17	32.44	< .001*
MASQ – AD	44.39 (10.22)	93.23 (9.02)	-18.36	48.47	< .001*

Note: AA = Anxious Arousal; AD = Anhedonic Depression; GDA = General Distress Anxious Symptoms; GDD = General Distress Depressive Symptoms; HAMD = Hamilton Depression Rating Scale; HC = Healthy control; MASQ = Mood and Anxiety Symptom Questionnaire; MDE = Major Depressive Episode; QIDS = Quick-Inventory of Depression; RRS = Ruminative Response Scale; SHAPS = Snaith-Hamilton Pleasure Scale; TRD = Treatment Resistant Depression

* = Statistical significance

Supplemental Table 2 – Medication class and usage of participants with treatment resistant depression.

Drug Class	Number of Participants	% of Participants
Anticonvulsant (including GABA analogues)	5	20.83
Anxiolytic/Sedative	5	20.83
Atypical Antipsychotic	11	45.83
Benzodiazepine	9	37.5
Central Nervous System Stimulant	6	25
Miscellaneous Antidepressant	6	25
Monoamine Oxidase Inhibitor (MAOi)	1	4.17
Serotonin Antagonist and Reuptake Inhibitor (SARI)	3	12.50
Serotonin-Noradrenaline reuptake inhibitor (SNRI)	5	20.83
Selective Serotonin Reuptake Inhibitor (SSRI)	12	50.00
Tri/Tetracyclic Antidepressant	2	8.33

Note: Most participants are taking multiple medications and so are counted in all relevant categories.

Supplemental Table 3 – Seed Coordinates (in Montreal Neurologic Institute space) for regions of interest in the Default Mode and Frontoparietal networks.

Network	*X*	*Y*	*Z*	Anatomical Structure
		DMN		
L DMN-A	–27	23	48	Superior frontal gyrus
R DMN-A	27	23	48	Superior frontal gyrus
L DMN-B	–41	–60	29	Angular gyrus
R DMN-B	41	–60	29	Angular gyrus
L DMN-C	–64	–20	–9	Middle temporal gyrus
R DMN-C	64	–20	–9	Middle temporal gyrus
Mid DMN-D	0	49	18	Medial frontal gyrus
L DMN-E	–25	–32	–18	Parahippocampal gyrus
R DMN-E	25	–32	–18	Parahippocampal gyrus
Mid DMN-F	0	–52	26	Posterior cingulate
		FPN		
L FPN-A	–40	50	7	Frontal pole
R FPN-A	40	50	7	Frontal pole
L FPN-B	–43	–50	46	Supramarginal gyrus
R FPN-B	43	–50	46	Supramarginal gyrus
L FPN-C	–57	–54	–9	Middle temporal gyrus
R FPN-C	57	–54	–9	Middle temporal gyrus
Mid FPN-D	0	22	47	Paracingulate gyrus
Mid FPN-E	0	4	29	Cingulate gyrus
Mid FPN-F	0	–76	45	Precuneus cortex

Note: Coordinates are reported in Montreal Neurological Institute space: X = left (-) to right (+), Y = posterior (-) to anterior (+), and Z = inferior (-) to superior (+). Anatomical labels are approximations.

DMN = Default Mode Network; FPN = Frontoparietal Network; L = Left Hemisphere; Mid = Midline; R = Right hemisphere

Supplementary Results

Global Connectivity

At the suggestion of a reviewer, we examined global lagged connectivity (GLC) to be able to further contextualise our ROI specific analysis. GLC is estimated using the following equation:

$$F_{Lag} = ln\frac{Det(R^{re}_{ZZ\omega})}{Det(R_{ZZ\omega})} = ln\frac{1-(r^{re}_{xy\omega})^2}{1-|r_{xy\omega}|^2} \quad (4)$$

Where $r_{xy\omega}$ is the complex-value coherence between the two timeseries, *x* and *y*, at a given frequency, ω, and *re* superscript denotes the real part of this matrix; see Section 3c and equations 3.7-3.13 of [6] for a full explanation of the derivation of this equation. Notably for this analysis, ω, was the central frequency of each of the investigated frequency bands, i.e., 5.75 Hz for Theta, 15.25 Hz for Beta1, 19.75 Hz for Beta2, 25.75 Hz for Beta3.

Turning to our analysis, in line with our main results, we first examined if GLC differed between the two groups at session 1 (i.e., pre-ketamine treatment for the TRD participants) using independent sample t-tests; subsequent ordinary least squares regression models were used to re-evaluate any identified significant group differences when also controlling for age. Across all frequency bands, we found that GLC did not differ between HCs and TRD (*t*'s ≤ 1.158, *p*'s ≥ .253) and this remained true even when controlling for age (*p*'s ≥ .492).

Next, we examined the putative group differences in the change in global connectivity (i.e., ΔGLC). Here, we found that TRD participants were characterized by a significantly larger change in beta3 ΔGLC (-0.20 ± 0.40 vs. 0.06 ± 0.57; $t = 2.055$, $p = .044$) even when controlling for group differences in age ($t = 2.068$, $p = .043$); ΔGLC in all other frequency bands did not differ significantly between groups (*p*'s ≥ .082).

Finally, we examined the between-session differences in GLC of each participant group. We observed that HC participants had no significant between-session change in GLC regardless of frequency bad (*p*'s ≥ .395). In contrast, we observed that the GLC of TRD participants significantly decreased in the Theta (6.03 ± 0.84 vs. 5.73 ± 0.82; $t = -2.55$, $p = .018$), Beta2 (6.42 ± 0.74 vs. 6.01 ± 0.77; $t = -2.748$, $p = .011$), and Beta3 (2.71 ± 0.55 vs. 2.51 ± 0.56; $t = -2.406$, $p = .025$) frequency bands.

Supplementary References

1. Hamilton M. A rating scale for Depression. J Neurol Neurosurg Psychiatry. 1960;23:56–62.
2. Clark LA, Watson D. Tripartite model of anxiety and depression: Psychometric evidence and taxonomic implications. J Abnorm Psychol. 1991;100:316–336.
3. Rush AJ, Trivedi MH, Ibrahim HM, Carmody TJ, Arnow B, Klein DN, et al. The 16-Item quick inventory of depressive symptomatology (QIDS), clinician rating (QIDS-C), and self-report (QIDS-SR): a psychometric evaluation in patients with chronic major depression. Biol Psychiatry. 2003;54:573–583.
4. Snaith RP, Hamilton M, Morley S, Humayan A, Hargreaves D, Trigwell P. A Scale for the Assessment of Hedonic Tone the Snaith–Hamilton Pleasure Scale. British Journal of Psychiatry. 1995;167:99–103.
5. Nolen-Hoeksema S, Morrow J. A prospective study of depression and posttraumatic stress symptoms after a natural disaster: The 1989 Loma Prieta earthquake. J Pers Soc Psychol. 1991;61:115–121.
6. Pascual-Marqui RD, Lehmann D, Koukkou M, Kochi K, Anderer P, Saletu B, et al. Assessing interactions in the brain with exact low-resolution electromagnetic tomography. Philosophical Transactions of the Royal Society A: Mathematical, Physical and Engineering Sciences. 2011;369:3768–3784.